P3.23 EVALUATION OF ANTARCTIC MESOSCALE PREDICTION SYSTEM (AMPS) FORECASTS FOR DIFFERENT SYNOPTIC WEATHER PATTERNS

Luna M. Rodriguez- Manzanet
University of Puerto Rico, Rio Piedras, Puero Rico

John J. Cassano*
University of Colorado, Boulder, Colorado

1. INTRODUCTION

Antarctica's combination of polar location and high elevation creates a unique environment. Antarctica is the coldest, highest, and driest continent on the planet. The average annual temperature in the interior is -50°C. The average elevation of the Antarctic surface is a little more than 2300 m, compared to Asia, the second highest continent with an average elevation of 800 m. The Antarctic plateau is one of the two largest deserts in the world receiving less than 8 cm of precipitation per year, in the form of snow. Despite the small annual precipitation less than 3% of Antarctica's 14 x 10^6 km^2 are free of snow or ice part of the year, and 75% of the total supply of fresh water on Earth exists in the form of ice, with 90% of this available stock lying in the huge ice load of this continent (Schwedtfeger 1984).

Antarctica is an important part of Earth's climate system; by acting as a global heat sink, it helps control our climate and weather. The high latitude of the Antarctic ice sheet limits the amount of solar insolation incident at the surface and the high reflectivity of the ice fields reduces the effective heating (Bromwich and Parish 1998). Antarctica modifies the earth's ocean because cold, dense, oxygen-rich water that originates in the Antarctic replenishes the ocean's supply of bottom water, contributing to the ocean's circulation.

Investigation of Antarctica will allow for a better understanding of how this ice-covered continent responds to environmental change. This knowledge will better enable us to predict the response of the Earth's climate system to future environmental changes.

*Corresponding author address: John J. Cassano, University of Colorado, CIRES / PAOS, 216 UCB, Boulder, CO 80309
e-mail: cassano@cires.colorado.edu

Logistical and scientific operations in Antarctica are susceptible to the harsh climate and rapid changes in the weather typical of this continent, and thus are critically dependent on accurate weather forecasts. These weather forecasts are produced by meteorologists who combine surface and upper air atmospheric observations, satellite data, and predictions from numerical weather prediction (NWP) models. Antarctica has few meteorological observations increasing the difficulty of making accurate weather forecasts. The extreme, unforgiving environment amplifies the risk stemming from poor forecast, while the sparse observing network often leaves forecasters heavily reliant on numerical weather prediction (NWP) guidance.

Under the support of the National Science Foundation (NSF), the Antarctic Mesoscale Prediction System (AMPS) has been providing real-time mesoscale NWP products for the Antarctic region since September 2000 (Powers et al. 2003). This system is built around the Polar Mesoscale Model 5 (Polar MM5), a version of the fifth generation Pennsylvania State University-National Center for Atmospheric Research Mesoscale Model adapted at the Byrd Polar Research Center at Ohio State University, for better performance in polar environments (Bromwich et al. 2001; Cassano et al. 2001).

This poster presentation and extended abstract describes an evaluation of the performance of AMPS forecasts for the Antarctic summer season of November, December, and January (NDJ). In order to evaluate AMPS performance the model predictions were compared with atmospheric observations from a number of automatic weather stations (AWSs) located on the Antarctic continent, and model validation statistics have been calculated. Unlike previous model validation projects we have calculated the model validation statistics for both seasonal time periods (NDJ) and also for different weather patterns. To the best of our knowledge this is a unique approach for model validation studies.

It is expected that the results from this project will benefit Antarctic weather forecasters by providing information on the skill of the AMPS model forecasts for a variety of weather conditions. Further, the results from this study will be useful for identifying shortcomings in AMPS and will identify aspects of the model that require additional model development in the future.

2. METHODS

We compared the AMPS predictions to observations made by University of Wisconsin automatic weather stations (AWS) located on the Ross Sea Ice Shelf (Figure 1). The AWS observations included temperature, pressure, wind speed and direction, and humidity. For this study only temperature, pressure, and wind speed were used.

As with all observational data the AWS dataset contained errors, and the first task before using the data was to analyze the data for errors. This error analysis was done by visually evaluating the raw 10-minute time series of the AWS data and looking for data values that were obviously in error (outliers in the data set or values outside of the reasonable range of values) (Figure 2). Next, the time series of the AWS data was plotted and compared to the AMPS predictions to provide a visual evaluation of the model forecast skill (Figure 4). Following, was the calculation of the model error statistics between the AWS data and the AMPS forecasts. The statistics that were calculated included the model bias (model mean minus AWS mean), the correlation coefficient (corr) between the AMPS and the AWS data, and the root-mean-square error (rmse). These statistics were calculated for all Antarctic summer months (November, December, and January) for which AMPS data were available (November 2001 through January 2003). Finally, we calculated the model error statistics for different synoptic weather patterns that occur during the Antarctic summer months. The time periods corresponding to the different weather patterns are based on an objective analysis scheme referred to as self-organizing maps, and the six weather patterns that were identified with this method are shown in Figure 3.

3. RESULTS AND DISCUSSION

Figures 4 through 7 show the results of the comparison of the AMPS forecasts and the AWS observations of pressure at the Ferrell AWS site. The time series of the observed and modeled pressure shown in Figure 4 indicates the generally high level of agreement between the modeled and observed pressure. The modeled pressure does show a slight offset from the observed pressure, but this is due to a difference in the actual elevation of the AWS site and the elevation of the model grid point corresponding to this site. The color-coding of the AWS time series is used to show how pressure varies for the six different weather patterns considered in this study.

In Figures 5 and 6 the mean of the AWS observed pressure is shown as a blue line. This mean is calculated for all of the NDJ observations (left most point on the curve) and for each of the six different weather patterns. As should be expected the mean pressure at the AWS site varies between the weather patterns, and this variation is consistent with sea level pressure fields shown in Figure 3. The lowest pressures at the AWS site are found for weather patterns 1x1 and 1x2, while higher pressure is found for the other weather patterns. The bias in the modeled pressure varies between approximately 4 and 6 mb and does not show a strong variation between the different weather patterns.

The RMSE increases as the forecast length increases, and this reflects the decrease in model forecast skill as the forecast duration increases (Figure 6). The RMSE is approximately 2 mb for the day 1 forecasts, but increases to values in excess of 6 mb by day 3. Also of interest in Figure 6 is the fact that the RMSE shows increasing variability between the different weather patterns as the forecast duration increases, with the largest RMSE found for weather patterns 1x2 and 2x1 at day 3.

The correlation coefficient is high for all three forecast time periods, with values greater than 0.8 (Figure 7). As should be expected the correlation coefficient does decrease as the forecast length increases, again showing a decrease in model skill with increased forecast duration.

Figures 8 and 9 show the AWS average temperature at Ferrell and Whitlock AWS sites, in a manner similar to what is shown in Figure 5 for the pressure at Ferrell. In both Figures 8 and 9 we notice that the temperature varies as the weather patterns change. The coolest temperatures are found for weather patterns 1x1 and 1x2 and the warmest temperatures are found for weather patterns 3x1 and 3x2. From Figure 3 we see that weather patterns 1x1 and 1x2 are associated with a strong low in the Ross Sea and that the circulation around this low results in strong flow from the interior of the Antarctic continent past both sites - thus leading to the cold temperatures. Weather patterns 3x1 and 3x2 are associated with a more maritime flow, and thus have warmer temperatures.

The model bias at both sites (Figures 8 and 9) becomes cooler with forecast time, and this has been found for other model studies of the AMPS model. Of interest is the fact that the day 1 bias at Ferrell is nearly 0 degrees C indicating that the model initial conditions are specifying an accurate temperature at this site. At Whitlock the day 1 bias is between +1.5 and 4 degrees C indicating that the model initialization is too warm at this location. Also from Figure 9 there is evidence that the model bias in temperature at Whitlock does vary with the weather patterns, with the model tending to be warmer for weather patterns 1x1 through 2x2 and cooler for the remaining two weather patterns.

Figure 10 shows the model RMSE for the Whitlock site. The RMSE is between 2 and 3 degrees C and does not vary appreciably either as a function of forecast duration or weather pattern. Figure 11 shows the correlation between the modeled and observed temperature at Whitlock. The correlation is relatively high, with values above 0.8 for most of the situations evaluated. Interestingly, the correlation is lowest for weather pattern 3x2.

The Whitlock site is located on a small island off the coast of the Ross Ice Shelf at an altitude of 275 m. The coarse resolution of the AMPS model does not allow for an accurate representation of this small island, or the elevation of this AWS site, and as a result some of the errors seen in Figures 9 through 11 may be due to this difference between reality and the model's representation of this location.

Figures 12 through 14 show the model validation results for the wind speed at Whitlock AWS site. The AWS average wind speed shown in both Figures 12 and 13 by the blue line indicate that the wind speed at this site varies from 2 to nearly 6 m/s depending on the weather pattern being considered. The strongest AWS average wind speeds are found for weather pattern 1x1, which corresponds to a strong low in the Ross Sea (Figure 3).

The model bias in the predicted wind speed is generally between -1 and +1 m/s, and does not vary appreciably between the different weather patterns considered (Figure 12). The RMSE varies from 2 to 4 m/s, with the largest RMSE occurring for weather pattern 1x2. Slightly smaller RMSE values are found for the weather patterns that have lower average wind speed at the AWS site.

The correlation between the model and AWS data is less than 0.7 for all forecast time periods and all weather patterns considered in this study (Figure 13). The correlation steadily decreases from weather pattern 1x1 to weather pattern 3x2. Given the general decrease in wind speed for these weather patterns, and the difficulty of accurately simulating weak wind conditions it is not surprising that the correlation is lowest for weather patterns 3x1 and 3x2.

4. CONCLUSIONS

With the unique approach of this model validation study we have evaluated the performance of AMPS forecasts for the Antarctic summer season. The results obtained from this project will benefit Antarctic weather forecasters by providing information on model performance for a variety of weather conditions and will be useful for identifying shortcomings in the AMPS model and will identify aspects of the model that require additional model development in the future.

Acknowledgments: This research was supported in part by NSF grants OPP-0229645 and ATM-9820037. Luna M. Rodriguez- Manzanet participation in this project was made possible by support from the University of Colorado Summer

Multicultural Access to Research Training program.

5. REFERENCES

Bromwich, D.H., J.J. Cassano, T. Klein, G. Heinemann, K.M. Hines, K. Steffen, and J.E. Box, 2001: Mesoscale modeling of katabatic winds over Greenland with the Polar MM5. *Mon. Wea. Rev.,* **129,** 2290-2309.

Bromwich, D.H. and Parish, T.R., 1998: Meteorology of the Antarctic. *Meteorology of the Southern Hemisphere*, Karoly, D.J. and D.G. Vincent (eds), American Meteorological Society, 410 pp.

Cassano, J.J., J.E. Box, D.H. Bromwich, L. Li, and K. Steffen, 2001: Evaluation of Polar MM5 simulations of Greenland's atmospheric circulation. *J. Geophys. Res.,* **106,** 33867-33890.

Powers, J.G., A.J. Monaghan, A.M. Cayette, D.H. Bromwich, Y.-H. Kuo, and K.W. Manning, 2003: Real-time mesoscale modeling over Antarctica: The Antarctic Mesoscale Prediction System. *Bull. Amer. Meteor. Soc.,* **84,** 1533-1545.

Schwedtfeger, W. 1984: *Weather and Climate of the Antarctic*. Elsevier, 261 pp.

6. FIGURES

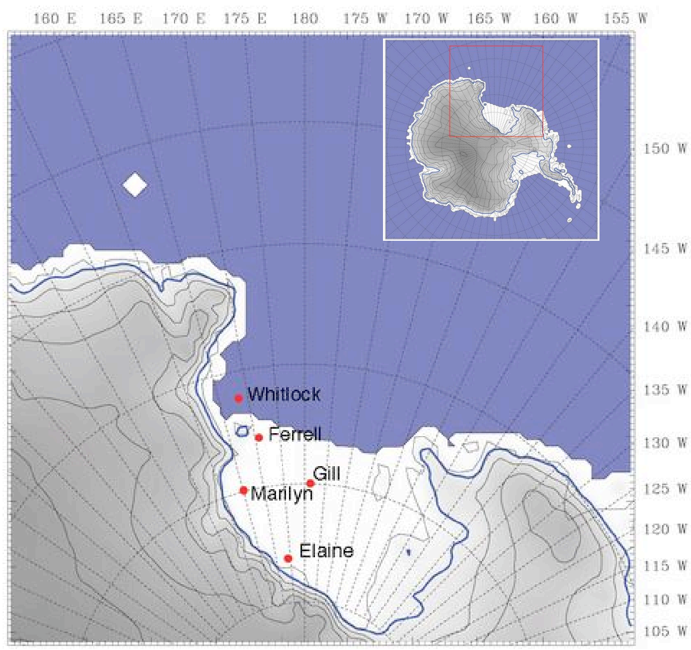

Figure 1: The locations of the AWS sites used for the model validation are shown. The inset map shows the portion of the Antarctic continent (inside the red box) that was used in the identification of the weather patterns.

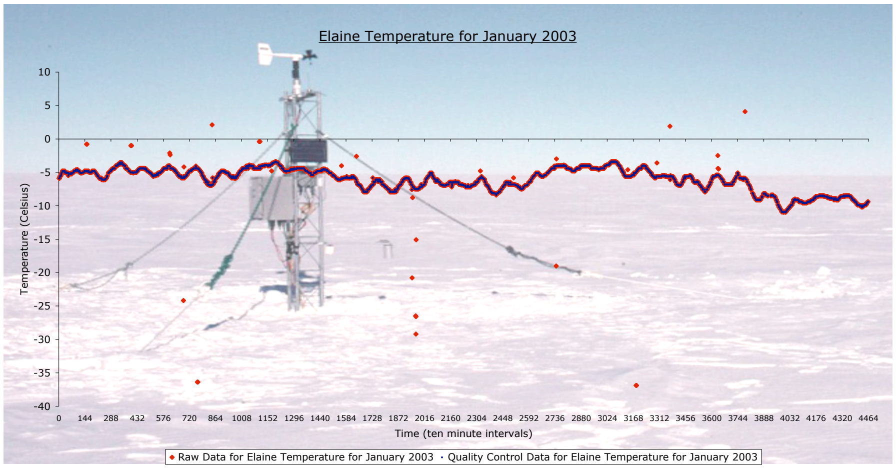

Figure 2: The time series of the raw (red symbols) and quality controlled (blue symbols) of temperature at the Elaine AWS site for January 2003. The background image is of Vito AWS on the Ross Ice Shelf.

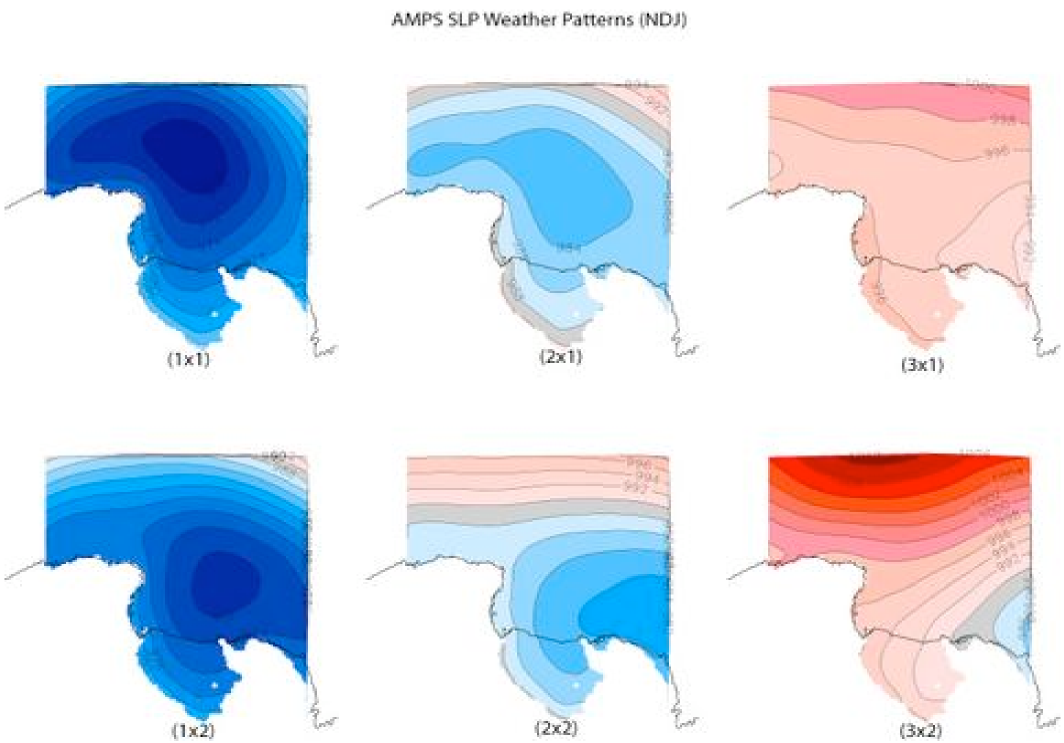

Figure 3: The SLP fields (colored contours) for the six weather patterns identified by the SOM analysis are shown. The labels below each weather pattern are used to identify the different weather patterns referred to in the text. The area shown in the plots is the same area as was shown in Figure 1.

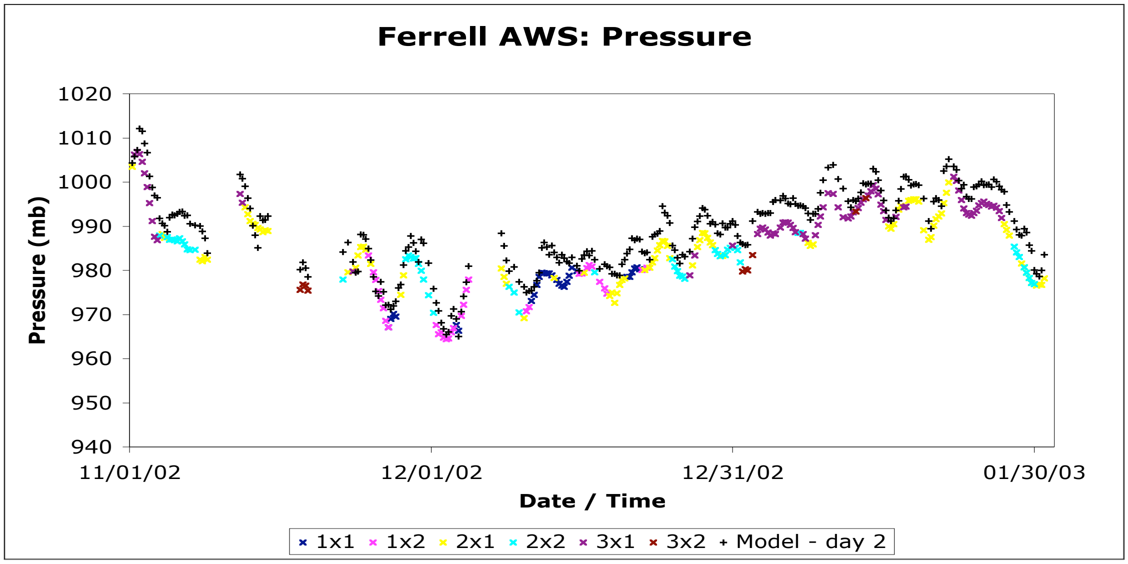

Figure 4: Time series of the modeled (black crosses) and observed (colored crosses) pressure at Ferrell site for November 2002 through January 2003. The model data is taken from the day 2 forecasts. The color-coding for the AWS data indicates the weather pattern identified for each observation time.

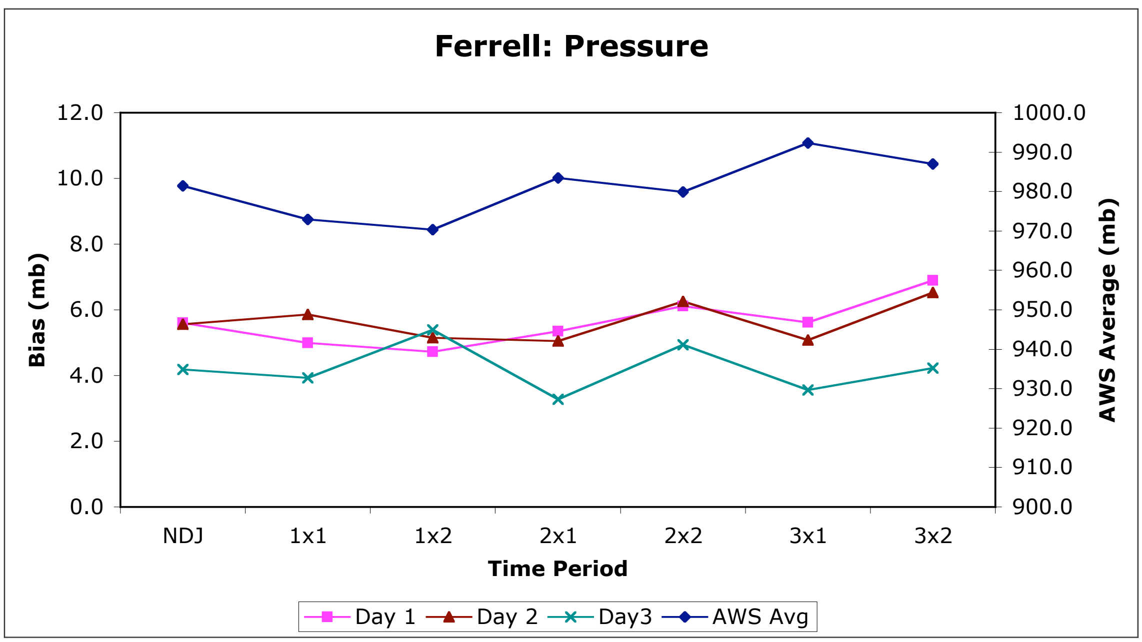

Figure 5: AWS (blue line with diamond symbols, right scale) and model bias (AMPS - AWS) (left scale) for AMPS day 1 (pink line with square symbols), day 2 (brown line with triangle symbols), and day 3 (turquoise line with cross symbols) pressure forecasts calculated for all NDJ observations and for each weather pattern at Ferrell site.

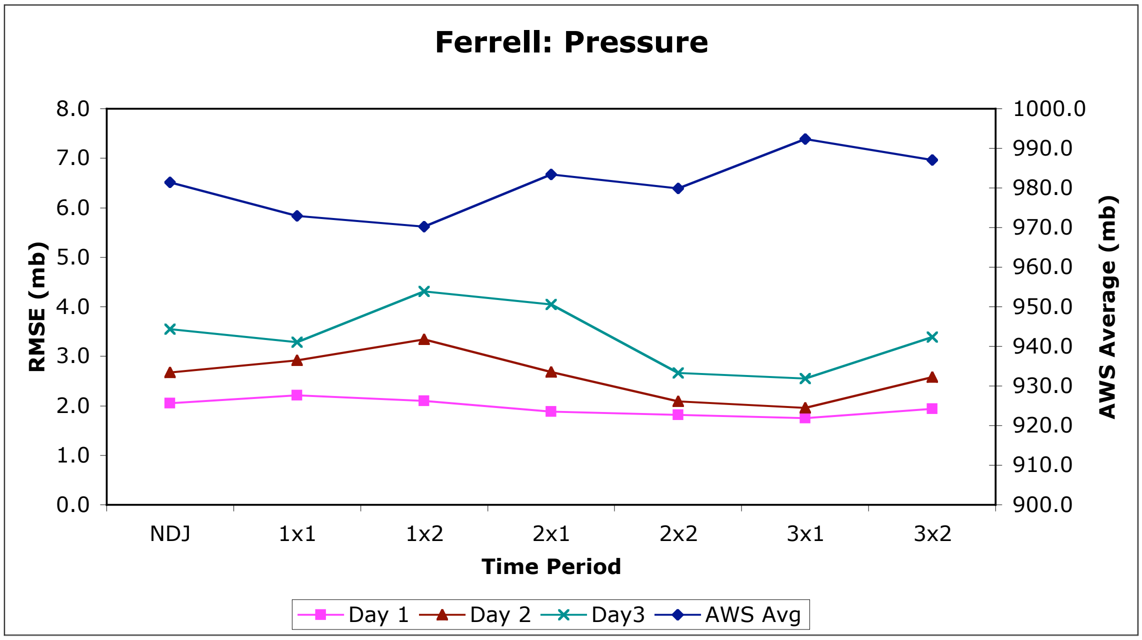

Figure 6: AWS (blue line with diamond symbols, right scale) and model rmse (left scale) for AMPS day 1 (pink line with square symbols), day 2 (brown line with triangle symbols), and day 3 (turquoise line with cross symbols) pressure forecasts calculated for all NDJ observations and for each weather pattern at Ferrell site.

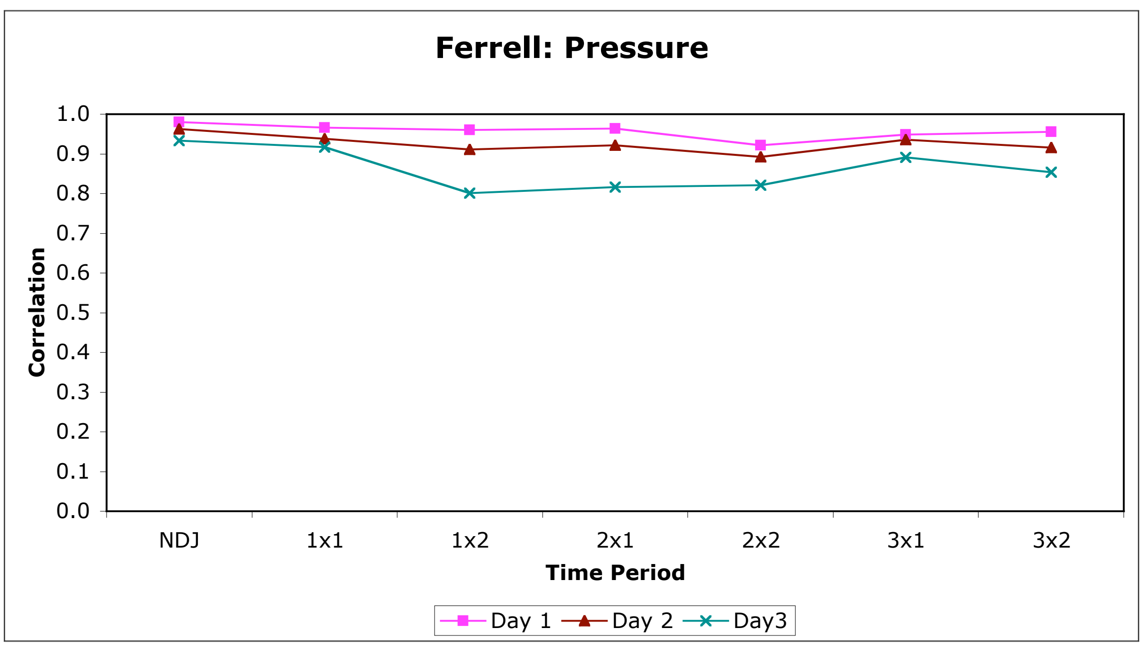

Figure 7: The correlation (measurement of the degree of linear relationship between the AMPS and the AWS data) of the model (left scale) of the pressure for AMPS day 1 (pink line with square symbols), day 2 (brown line with triangle symbols), and day 3 (turquoise line with cross symbols) pressure forecasts calculated for all NDJ observations and for each weather pattern at Ferrell.

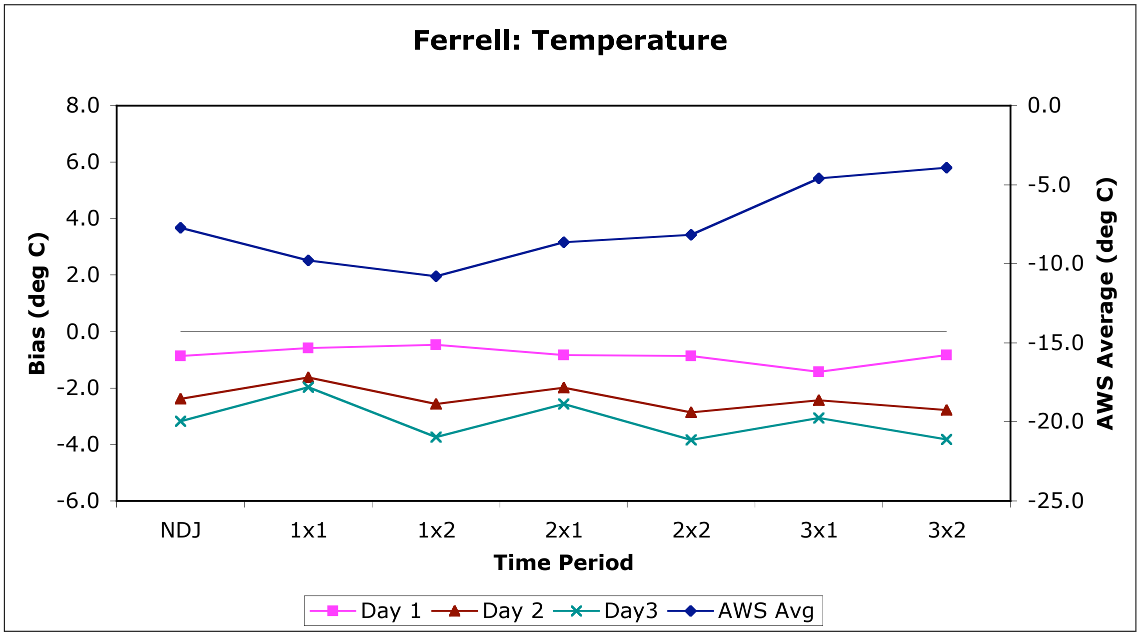

Figure 8: AWS (blue line with diamond symbols, right scale) and model bias (AMPS - AWS) (left scale) for AMPS day 1 (pink line with square symbols), day 2 (brown line with triangle symbols), and day 3 (turquoise line with cross symbols) temperature forecasts calculated for all NDJ observations and for each weather pattern at the Ferrell site.

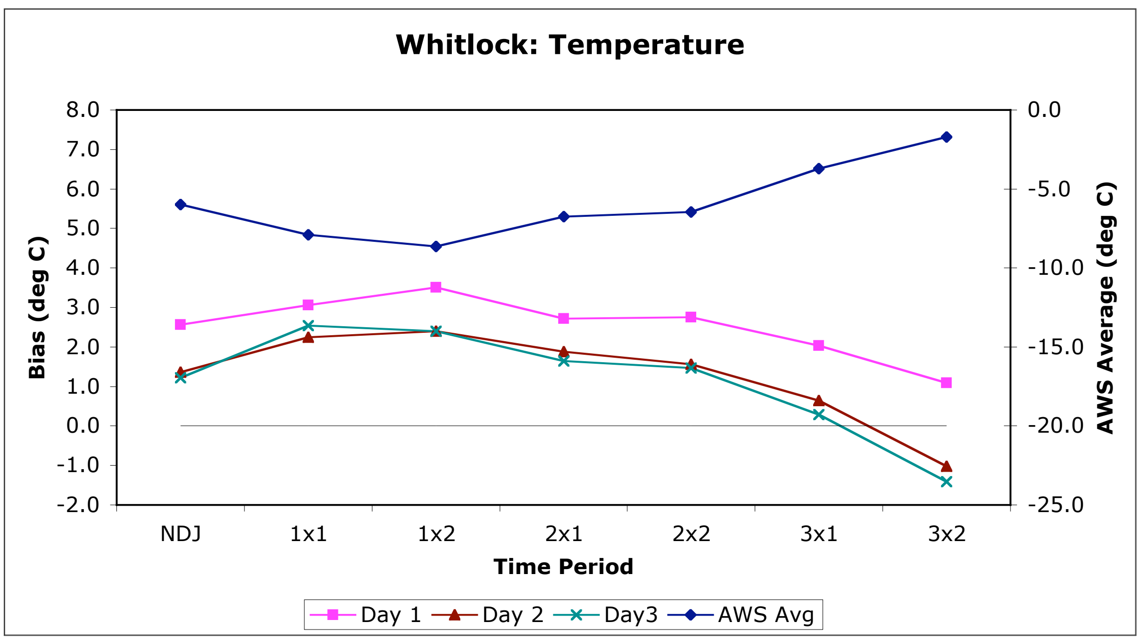

Figure 9: AWS (blue line with diamond symbols, right scale) and model bias (AMPS - AWS) (left scale) for AMPS day 1 (pink line with square symbols), day 2 (brown line with triangle symbols), and day 3 (turquoise line with cross symbols) temperature forecasts calculated for all NDJ observations and for each weather pattern at the Whitlock site.

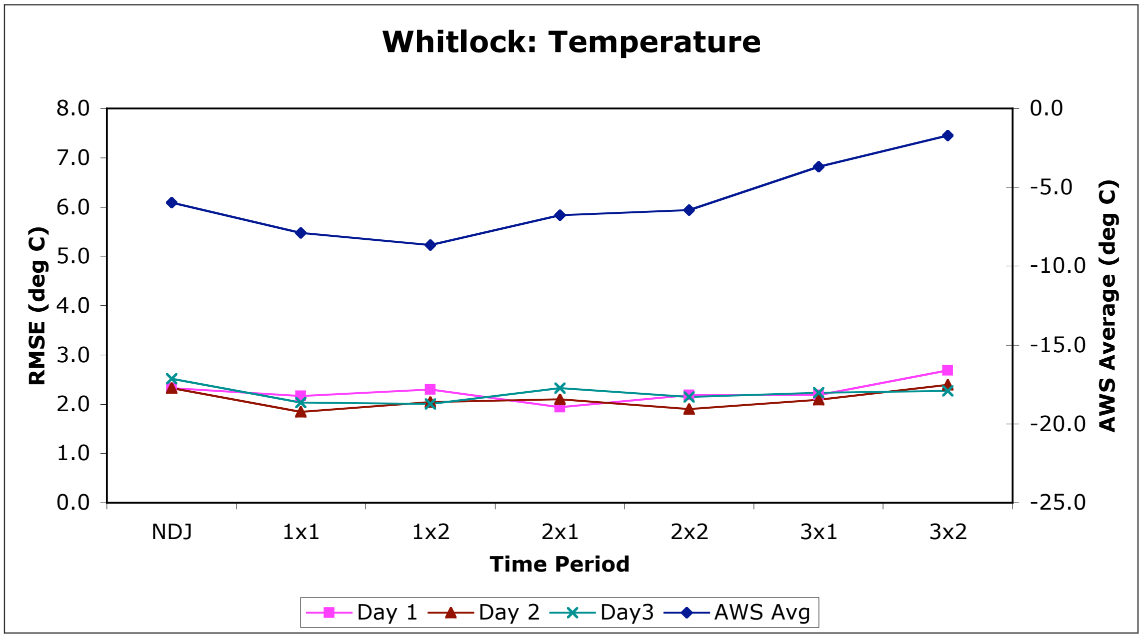

Figure 10: AWS (blue line with diamond symbols, right scale) and model rmse (left scale) for AMPS day 1 (pink line with square symbols), day 2 (brown line with triangle symbols), and day 3 (turquoise line with cross symbols) temperature forecasts calculated for all NDJ observations and for each weather pattern at the Whitlock site.

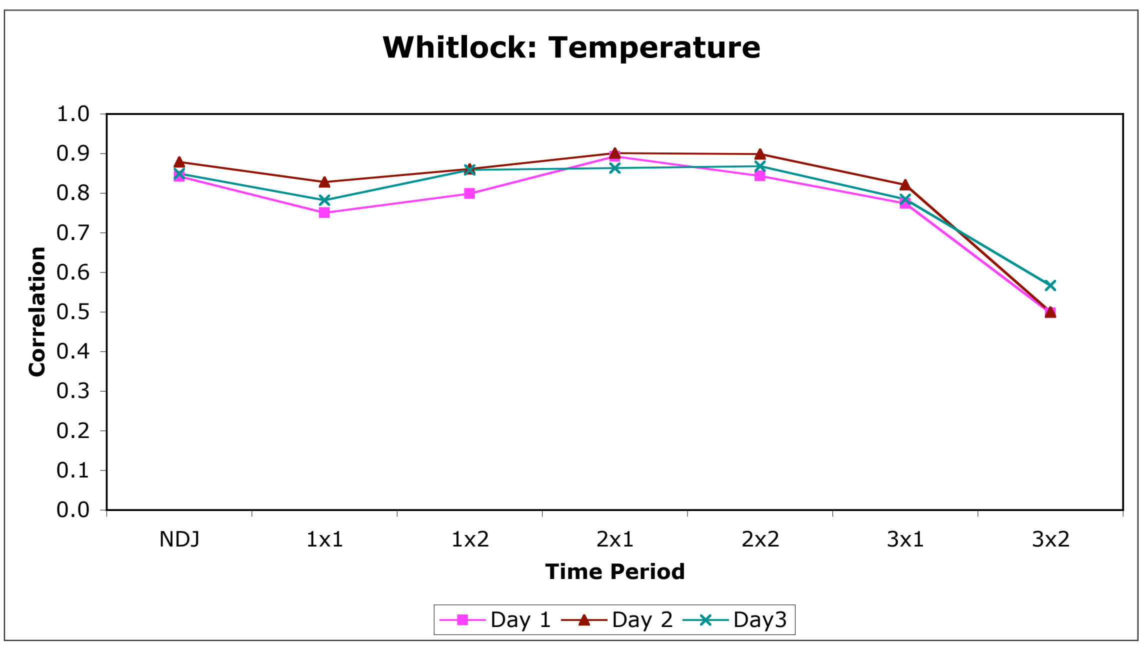

Figure 11: The correlation coefficient of the modeled and observed (left scale) temperature for AMPS day 1 (pink line with square symbols), day 2 (brown line with triangle symbols), and day 3 (turquoise line with cross symbols) temperature forecasts calculated for all NDJ observations and for each weather pattern at Whitlock.

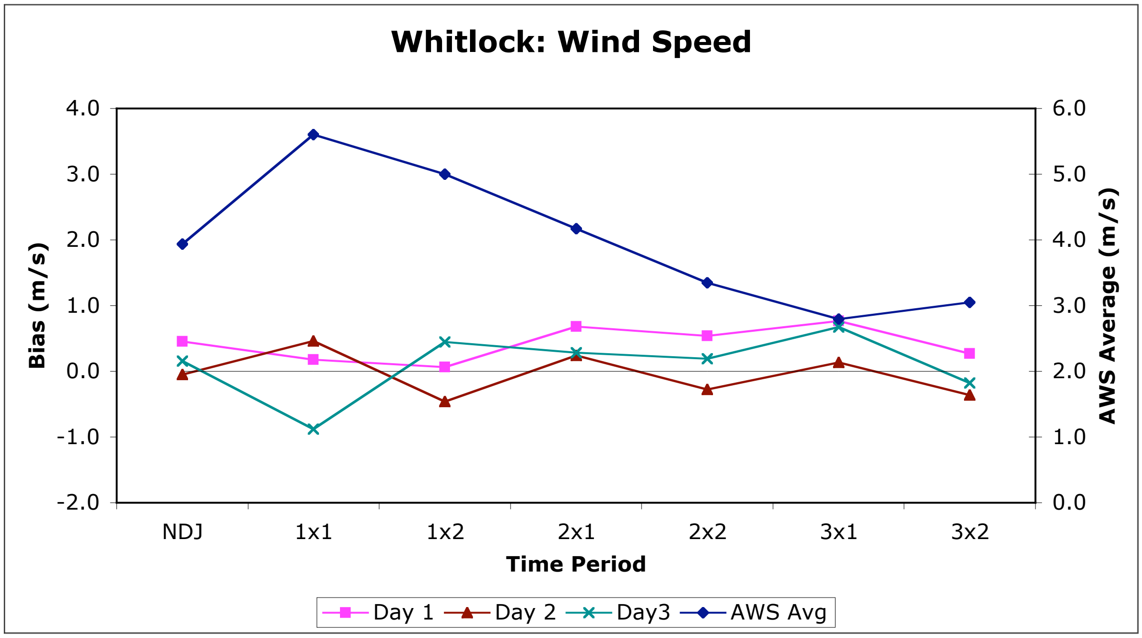

Figure 12: AWS (blue line with diamond symbols, right scale) and model bias (AMPS - AWS) (left scale) for AMPS day 1 (pink line with square symbols), day 2 (brown line with triangle symbols), and day 3 (turquoise line with cross symbols) wind speed forecasts calculated for all NDJ observations and for each weather pattern at the Whitlock site.

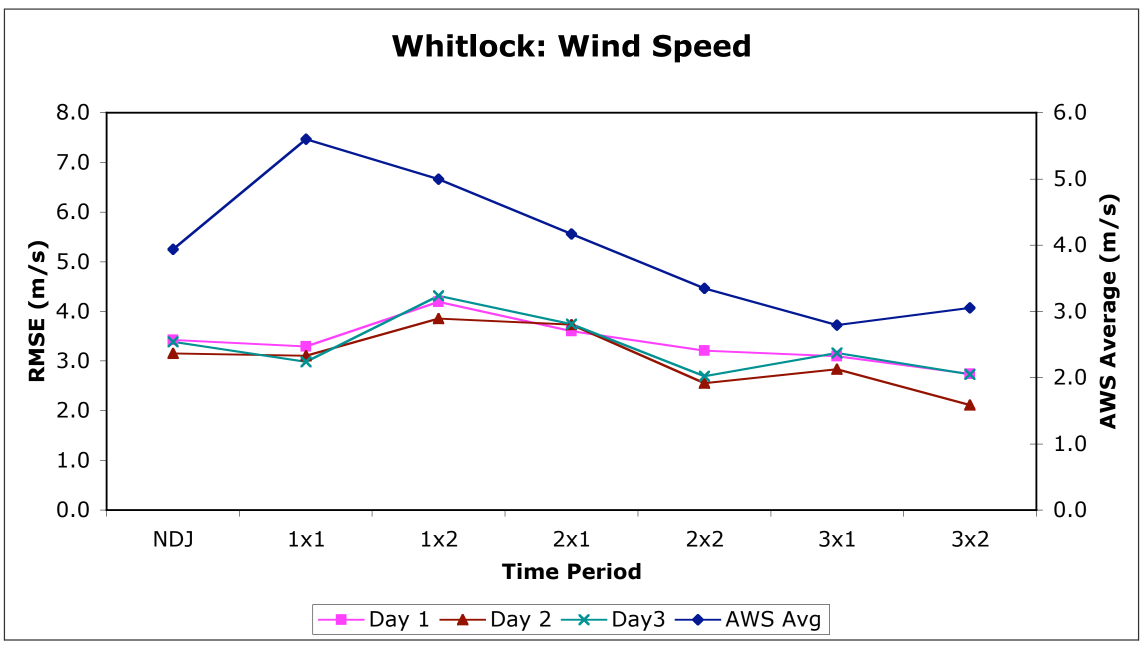

Figure 13: AWS (blue line with diamond symbols, right scale) and model rmse (left scale) for AMPS day 1 (pink line with square symbols), day 2 (brown line with triangle symbols), and day 3 (turquoise line with cross symbols) wind speed forecasts calculated for all NDJ observations and for each weather pattern at Whitlock site.

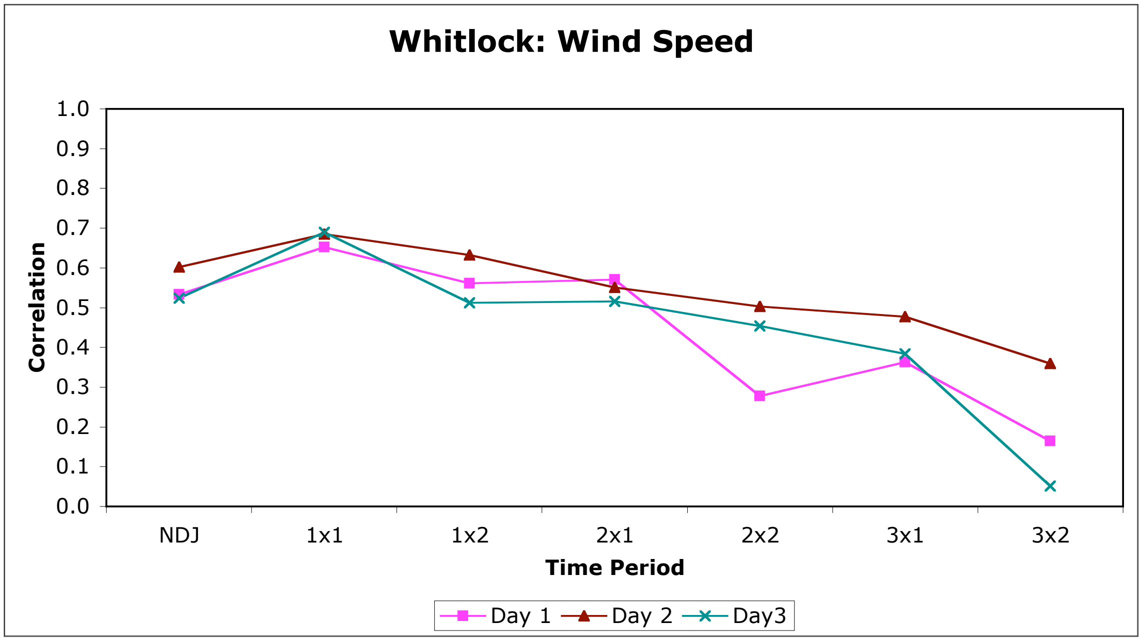

Figure 14: The correlation coefficient of the modeled and observed (left scale) wind speed for AMPS day 1 (pink line with square symbols), day 2 (brown line with triangle symbols), and day 3 (turquoise line with cross symbols) wind speed forecasts calculated for all NDJ observations and for each weather pattern at Whitlock.